Results of the 2001 JPL Balloon Flight Solar Cell Calibration Program

B. E. Anspaugh
R. L. Mueller

March 1, 2002

Results of the 2001 JPL Balloon Flight Solar Cell Calibration Program

B. E. Anspaugh
R. L. Mueller

March 1, 2002

ABSTRACT

The 2001 solar cell calibration balloon flight campaign consisted of two flights, which occurred on June 26, 2001, and July 4, 2001. Fifty-nine modules were carried to an altitude of $\approx$ 120,000 ft (36.6 km). Full I-V curves were measured on nineteen of these modules, and output at a fixed load was measured on thirty-two modules (forty-six cells), with some modules repeated on the second flight. Nine modules were flown for temperature measurement only. The data from the fixed load cells on the first flight was not usable. The temperature dependence of the first-flight data was erratic and we were unable to find a way to extract accurate calibration values. The I-V data from the first flight was good, however, and all data from the second flight was also good. The data was corrected to 28°C and to 1 AU (1.496 $\times$ 10^8 km). The calibrated cells have been returned to their owners and can now be used as reference standards in simulator testing of cells and arrays.

ACKNOWLEDGMENTS

CONTENTS

Tables

"Balloons! The emotions that word brings to life! The tiny balloons of the amusement parks are the silent bubbles of children's thought, their fairy tales and dreams. The others, the big ones, contain romance, nostalgia, adventure, and comedy. Something for dreamers and philosophers, artists and writers. And, at the same time, a serious challenge for technicians and scientists." *The Art of Ballooning* by Peter Anderson and Torleif Svensson

1. INTRODUCTION AND OVERVIEW

The primary source of electrical power for robotic space vehicles is the direct conversion of solar energy through the use of solar cells. As advancing cell technology continues to modify the spectral response of solar cells to utilize more of the Sun's spectrum, designers of solar cells and arrays must have the capability of measuring these cells in a light beam that is a close match to the solar spectrum. The solar spectrum has been matched closely by laboratory solar simulators. But the design of solar cells and the sizing of solar arrays require such highly accurate measurements that the intensity of these simulators must be set very accurately. A small error in setting the simulator intensity can conceivably cause a disastrous missizing of a solar panel, causing either a premature shortfall in power or the launch of an oversized, overweight solar panel.

The Jet Propulsion Laboratory (JPL) solar cell calibration program was conceived to produce reference standards for the purpose of accurately setting solar simulator intensities. The concept is to fly solar cells on a high-altitude balloon, to measure their output at altitudes near 120,000 ft (36.6 km), to recover the cells, and to use them as reference standards for setting solar simulator intensities. This is done by placing the reference cell in the simulator beam, then adjusting the beam intensity until the reference cell reads the same as it read on the balloon. As long as the reference cell has the same spectral response as the cells or panels to be measured, this is a very accurate method of setting the intensity. But as solar cell technology changes, the spectral response of the solar cells changes also, and reference standards using the new technology must be built and calibrated.

Until the summer of 1985, there had always been a question as to how much the atmosphere above the balloon modified the solar spectrum. If the modification was significant, the reference cells might not have the required accuracy. Solar cells made in recent years have increasingly higher blue responses; if the atmosphere has any effect at all, it would be expected to modify the calibration of these newer blue cells much more than for cells made in the past.

In late 1984, a collection of solar cells representing a wide cross section of solar cell technology was flown on the shuttle Discovery as a part of the Solar Cell Calibration Facility (SCCF) experiment. The cells were calibrated as reference cells on this flight by using procedures similar to those used on the balloon flights. The same cells were then flown on the 1985 balloon flight and remeasured. The 2 sets of measurements gave nearly identical results (see reference 1), thus verifying the accuracy of the calibration procedures used on the balloon flights.

JPL has been flying calibration standards on high-altitude balloons since 1963 and continues to organize a calibration balloon flight at least once a year. The 2001 balloon flights were the 59th and 60th flights in the series. The 2001 flights incorporated a total of 59 solar cell modules. There was a total of 9 different participants, including JPL. The payload included Si, GaAs, GaAs/Ge, Ge, and multi-junction cells, along with top, middle, and bottom sections of dual and triple-junction cells.

A new data acquisition system was built for the balloon flights and flown for the first time on the 1995 flight. This system allows the measurement of current-voltage (I-V) curves for 19 modules, in addition to measurement of modules with fixed loads, as had been done in the past.

The Sun angle sensor, first flown in 1996, was flown on the 2001 flights. This sensor measures the angle of the Sun in both azimuth and elevation and adds this information to the telemetry stream using 4 of the fixed-cell data channels.

2. PREFLIGHT PROCEDURES

2.1 MODULE FABRICATION

The cells were mounted by the participants or by JPL on JPL-supplied standard modules in accordance with standard procedures developed for the construction of reference cells. The JPL standard module is a machined

1

copper or aluminum block on which a fiberglass circuit board is mounted. The circuit board has terminals that are used for making electrical connections to the solar cell and to a load resistor. On those cells slated for I-V measurement, no load resistor is connected. The circuit boards include 2 binding posts and a jumper in series with one of the leads to the resistor. After flight calibration, the jumper can be removed and replaced with current pickoff probes for use on those pulsed xenon simulators that require a current input. The cell current (mA) will then be equal to the cell calibration value (mV) divided by the load resistance. The assembly is painted with either high-reflectance white or low-reflectance black paint.

The resistor on the fixed-load cells performs 2 tasks. First, it loads the cells near short-circuit current (I_{sc}), which is the cell parameter that varies in direct proportion to light intensity. Second, it scales the cell outputs to read slightly less than 100 mV during the flight, the maximum input voltage allowed by the data acquisition electronics for the fixed-load cells. Load resistance values are chosen to match the electrical characteristics of each cell flown. Nominally, the resistors will be ≈ 0.5 ohm for a 2 $\times$ 2 cm Si cell, 0.66 ohm for a 2 $\times$ 2 cm GaAs cell, 0.25 ohm for a 2 $\times$ 4 cm Si cell, etc. The load resistors are precision resistors (1.0%, 20 ppm/°C) and have a resistance stability equal to or better than $\pm 0.002\%$ over a 3-year period. The solar cell modules built by JPL utilize a silicone elastomer (CV2568 from Nusil Silicone Technology) to glue the cells to the body of the machined metal block. This gives a good thermal conductivity path between the cells and the metal blocks, while providing electrical insulation between the rear surface of the solar cells and the block.

2.2 CELL MEASUREMENTS

After the cells were mounted on the blocks, the electrical output of each cell module was measured under illumination by the JPL X25 Mark II solar simulator. For these measurements, the simulator intensity was set by using only a reference cell that was judged to closely approximate the spectral response of the individual flight module. The absolute accuracy of these measurements is somewhat uncertain, but the measurements do allow checking of the modules for any unacceptable assembly losses or instabilities. After the balloon flight, the cells were measured in exactly the same way to check for any cell damage or instabilities that may have occurred as a result of the flight.

2.3 TEMPERATURE COEFFICIENTS AND LEAST SQUARES FITS

The temperature coefficients of the mounted cells were also measured before the flight. The modules were mounted in their flight configuration on a temperature-controlled block in a vacuum chamber. Cell outputs were measured at 25, 35, 45, 55, 65, and 75°C under illumination with the X25 simulator. The temperature coefficients of the fixed-cell cell modules were computed by fitting the output vs temperature relationship with a linear least squares fit. Temperature coefficients for the I-V cells were computed using a linear least squares fit to both the short-circuit current and open-circuit voltage (V_{oc}) data.

The data analysis program was modified in 1998 to allow the measurement of cell temperature coefficients using the flight data. When the tracker first locks on the Sun after reaching float altitude during the flight, the cell temperatures are between 30° and 40°C, depending on the time of launch. As the flight progresses, the cell temperatures rise to ≈ 75°C. This data was used to compute temperature coefficients both for the fixed-load cells and for the I-V cells. In the latter case, temperature coefficients for both I_{sc} and V_{oc} were computed. The temperature coefficients measured during the flight were compared with those measured with the X25, and those that seemed to give the best fits to the data were used for the analysis.

2.4 DATA ACQUISITION SYSTEM CHECKOUT AND CALIBRATION

The 1995 data acquisition (DAQ) system was used for the calibration measurements on the 2001 flights. This system is based on a 286 microprocessor in a ROM-DOS operating system. The program that controls the system is easily changed to match the requirements of each individual flight. This system also duplicates the function of the older data encoder with regard to reading and processing the outputs of the modules with fixed-load resistors (maximum input voltage of 100 mV). The system has 7 dedicated temperature measurement channels, 6 for the panel and 1 for the internal DAQ temperature. The temperature sensors now in use are platinum resistance sensors (RTDs), which are embedded under the solar cells in the modules dedicated to temperature measurement. The system has the capability of measuring the I-V characteristics of as many as 19 solar cells and 1 reference channel. Loading of the cells to produce the I-V curves is accomplished by applying 20 resistive loads, 1 at a time, to each cell and measuring the cell's output voltage and current as each load is applied.

2

Each cell has its own individually tailored set of 20 load resistors. The resistive loads are chosen to generate the expected I-V characteristic of each cell and to produce a large number of points near the maximum power (P_{max}) point. Sixteen resistors are available for cell loading. Selection of these resistors in parallel combinations of up to 5 at a time results in a theoretical total of 6,884 possible resistive loads (although this number includes many duplicates) available for each cell. A 4-wire system is used for the I-V measurements, so that the wires measuring cell voltage do not carry current.

The heart of the DAQ is a 286-class computer on an STD bus circuit board. This computer controls the multiplexing of the cells data, temperature data, calibration voltages, and power supply voltages for measurement. The computer is also used to connect each I-V cell in its turn to the measurement circuitry, and the computer also applies the tailored set of load resistors across the cell under measurement. The computer is used to format the data, to add clock time, synch words, and a checksum for each line, and then to send all of this to the telemetry transmitter via an RS232 output at a rate of 9600 baud. All of the test and measurement parameters are read out and transmitted during the course of a telemetry frame. During this time the fixed-load cells are each read 5 times, and each of the I-V cells is read once. All other engineering voltages and temperatures are also read once each frame. As presently programmed, a telemetry frame is sent every 9.5 seconds.

All measurements of electrical parameters are performed by sending the signals through suitable amplifiers, and then to a 12-bit A/D converter. The fixed-load cell signals are sent through an amplifier with a gain of 49.7716. The I-V cell voltage levels are sent through an amplifier with a gain of 1.7663. (Note: This amplifier was decreased from its previous value of 2.0 to accommodate the higher open-circuit voltages produced by modern dual- and triple-junction cells.) Cell currents were passed through a precision 0.1-ohm resistor. The voltage drop across this resistor was fed to a differential amplifier with a system (resistor plus amplifier) gain of 5.2734 volts/amp. These gains were measured by connecting a series of voltages (or currents) into the multiplexer feeding each amplifier and measuring the output voltage. These gains are measured each year either before or after the flight(s). The repeatability of the gain measurements to date has been better than 0.03% for the voltage amplifiers and better than 0.17% for the current amplifier. The on-Sun indicator and the 7 temperature signals were each sent through individual amplifiers. These amplifiers were also individually calibrated prior to flight. Calibration voltages were built into the DAQ and are used for monitoring the gain and

stability of the voltage amplifiers during the flight. Three calibration voltages of approximately 50, 80, and 100 mV from an external voltage reference source housed in the DAQ box are also multiplexed into the data stream as a cross-check on the system. The Sun-angle-sensor data was sent through 4 of the fixed-load channels and incorporated into the telemetry stream.

The program was modified in 1999 to calculate the gain of the fixed-load-cell amplifier continuously during the flight. The known, stable voltages from the external voltage reference source were used as input, and the telemetered output values were used as output. A linear least squares fit routine was used to calculate the gain and offset of the amplifier continuously during the flight.

The program was again modified in 2000 to allow the option of calculating the gain of the fixed-load-cell amplifier using internal calibration voltages of ≈ 50 and 90 mV built into the DAQ. This option also permits calculating the gain and offset of the amplifier continuously during the flight.

The system is designed so that the output from the DAQ on the RS232 line can be fed directly to the COM input of a PC for preflight testing. During the flight, the line connecting the RS232 output to the PC is replaced with connections to a telemetry transmitter and a telemetry receiver. Since the overall system operation is equally effective whether the connection is by cable or by radio, this configuration allows a much more thorough checkout of the system before it leaves JPL and during the various preflight checkouts at the National Scientific Balloon Facility (NSBF) at Palestine, Texas.

The PC program for receiving, converting, and storing data is written in LabVIEW, a graphical programming language specifically designed for making engineering-type measurements under PC control. The LabVIEW program provides for graphical display of the outputs from all the fixed-load cells simultaneously. The I-V curves of any or all of the 19 I-V cells may also be displayed. The program provides for digital readout of all power supply voltages, calibration voltages, temperatures, and on-Sun indicator readings. The Sun-angle-sensor data is displayed in the form of a scatter plot on the LabVIEW display. Synch status and checksum status are continuously displayed. These displays are continuously updated in real time and give an instantaneous reading on the status of the whole system.

2.5 PANEL ASSEMBLY AND CHECKOUT

After the electrical measurements of the solar cells were completed, the modules were mounted on the solar panel and connected electrically. Figure 1 is a photograph of the mounted modules for the first 2001 flight, Figure 2 is a diagram of the panel that identifies the modules by their serial numbers, and Figure 3 is a photograph of the tracker and panel after it was later mounted on the hoop assembly at Palestine. Figures 4, 5, and 6 show similar views of the assemblies for the second 2001 flight. After completion of the panel assembly, the panel, tracker, and DAQ were all given complete functional tests in terrestrial sunlight. The assembled tracker and panel were placed in sunlight on a clear, bright day and checked for the tracker's ability to acquire and track the Sun while each cell module was checked for electrical output. All power supply voltages and temperature readings were checked, and the calibration voltages were checked for stability and proper function. After these tests were completed satisfactorily, the assembly was shipped to NSBF for flight.

2.6 PRELAUNCH PROCEDURES AT PALESTINE

The NSBF was established in 1963 at Palestine, Texas. This location was chosen because it has favorable weather conditions for balloon launching and a large number of clear days with light surface winds. The JPL calibration flights have flown from the Palestine facility since 1973. The flights are usually scheduled in the June-to-September time period, since the Sun is high in the sky at that time of year and the sunlight passes through a minimum depth of atmosphere before reaching the solar modules. Also, the high-altitude winds in this time period take the balloons over the sparsely populated areas of east Texas, so the descending payloads are unlikely to cause damage to persons or property.

Upon arrival at Palestine, the tracker and module payload were again checked for proper operation. This included a checkout in an environmental test chamber wherein the tracker, calibration voltages, and the entire data acquisition system were all tested as a system. The chamber was pumped down to a pressure of ≈ 5 mbar (0.05 N/cm^2), then backfilled with dry nitrogen to a pressure of ≈ 800 mb. The DAQ was then cooled to $-40°$C. The system was tested at $10°$ increments during the cooldown. The system was pumped down to a pressure of 5 mbar (corresponding to an altitude of 118,000 ft) and soaked for 30 minutes at this temperature and pressure. Following this, the chamber was backfilled with dry nitrogen and warmed up to $+50°$C, with tests occurring at each $10°$ increment. Then the assembly was removed from the environmental chamber, and a room-temperature, end-to-end check was performed on the payload, telemetry, receiving, and decoding systems.

After all the checkouts and calibrations were performed, the tracker was mounted on an aluminum tubular hoop structure. This assembly was then mounted on the top portion (or apex) of the balloon. Figures 3 and 6 are photographs of the tracker mounted on the hoop assembly for the first and second 2001 flights. The solar panel is shown as it was configured for the 2 flights.

3. BALLOON SYSTEM

The main components of the balloon flight system are (1) the apex-mounted hoop assembly that contains the experimental package, the data encoder, the command receiver, the data telemetry system, and the recovery system; (2) the balloon; and (3) the lower payload that contains the terminate system, the Global Positioning System (GPS) receivers, transponder, and the housekeeping telemetry system and command receiver for the balloon system. There was a major change in the design of the balloon system in 1997. A special telemetry system was designed specifically for the top payload. This system consists of a command receiver, data telemetry transmitter, and a transmitter for sending housekeeping data for the top payload. These items, along with the batteries to power them, are all installed on the hoop assembly. The main balloon system has its own command receivers and telemetry transmitters as before, but the two systems are now completely isolated from each other. This new design was implemented in order to eliminate the long cables running from the top of the balloon to the systems at the bottom gondola, as it was suspected that these long cables behaved like antennas capable of picking up electrostatic charges and inducing flight failures.

A color TV camera was added to the top payload assembly in 1998. This camera, along with its dedicated transmitter and battery supply, allows the team to view the operation of the tracker in real time during the flight. The images are recorded on a VCR in the NSBF control tower.

3.1 BALLOON DESCRIPTION

The balloons used for the JPL solar cell calibration high-altitude flights are manufactured by the Winzen Balloon Group of Raven Industries. The balloons have a volume of 3.46 million ft^3 (98,000 m^3). The balloon manufacturer uses 0.8-mil (20-μm) polyethylene film (Stratofilm-372) designed specifically for balloon use.

Figure 1.   Photograph of the 2001-1 Balloon Flight Solar Panel

Figure 2. Module Location Chart, 2001-1 Flight

Figure 3. Tracker Mounted on Aluminum Hoop Assembly for 2001-1 Flight

Figure 4.   Photograph of the 2001-2 Balloon Flight Solar Panel

SUN ANGLE SENSOR

JPL 97-006 (T6) 28	JPL 86-023 40

Boeing 01-160 37

JPL 01-006A 35

Tecstar 01-131 36 | JPL 01-189A 38 | 01-189B 39

JPL 97-004 (T5) 43

ON SUN

MSFC 01-194A 41 | MSFC 01-194B 42

MSFC 01-193A 33 | 01-193B 34

MSFC 01-191A 31 | 01-190B 01-193B 32

JPL 97-003 (T4)

JPL 73-182 27

JPL 01-190A 29 | 01-190B 30

Emcore 01-101 26

Tecstar 01-139 24

Boeing 01-169 23

SPL 01-158 9

Tecstar 01-126 25

JPL 95-004 (T3) 10

Boeing 01-163 22

JPL 95-003 (T2)

R. Robin No. 25 2

Emcore 01-106 21

Boeing 01-174 1

SPL 01-151A 01-152A 7 | 01-151B 01-152B 8

SPL 01-151A 5 | 01-151B 6

SPL 01-150A 3 | 01-150B 4

JPL 97-002 (T1)

(T1) -- (T6) RTDs
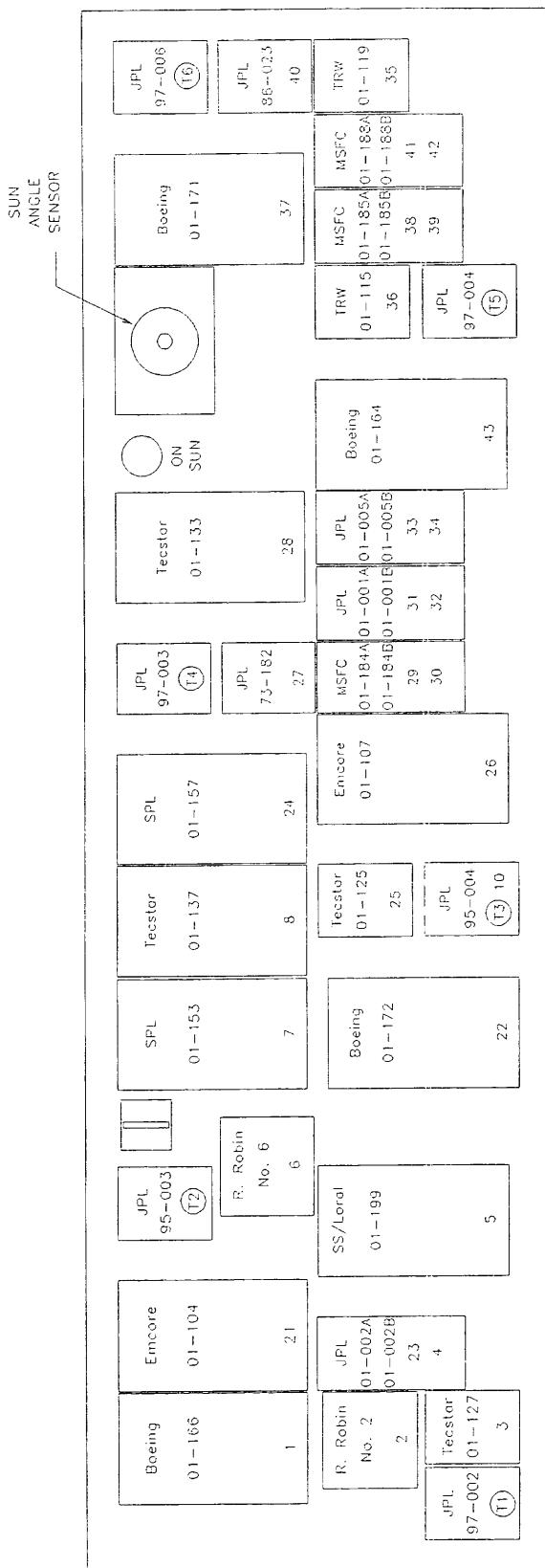
9

Figure 5. Module Location Chart, 2001-2 Flight

Figure 6. Tracker Mounted on Aluminum Hoop Assembly for 2001-2 Flight

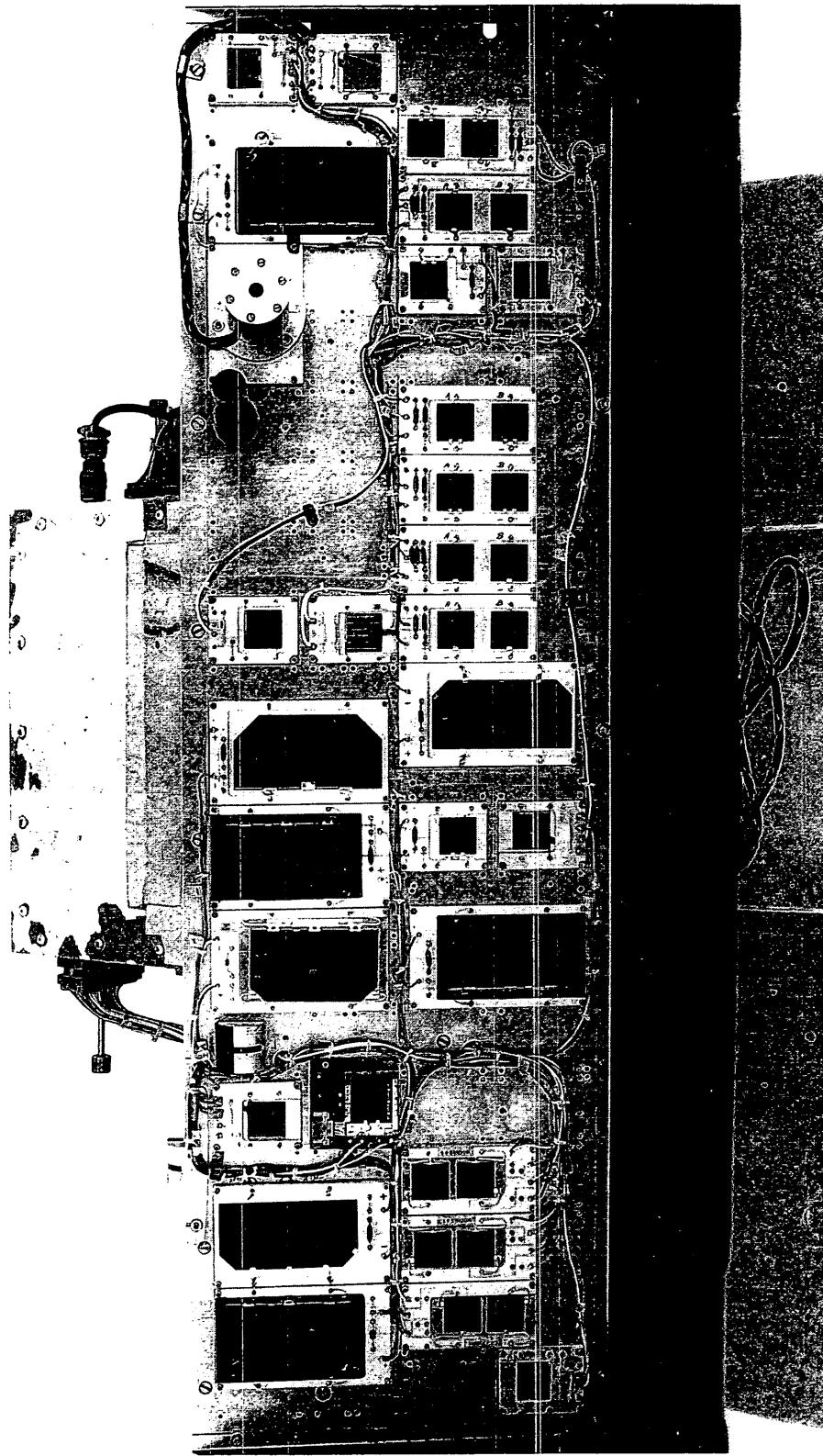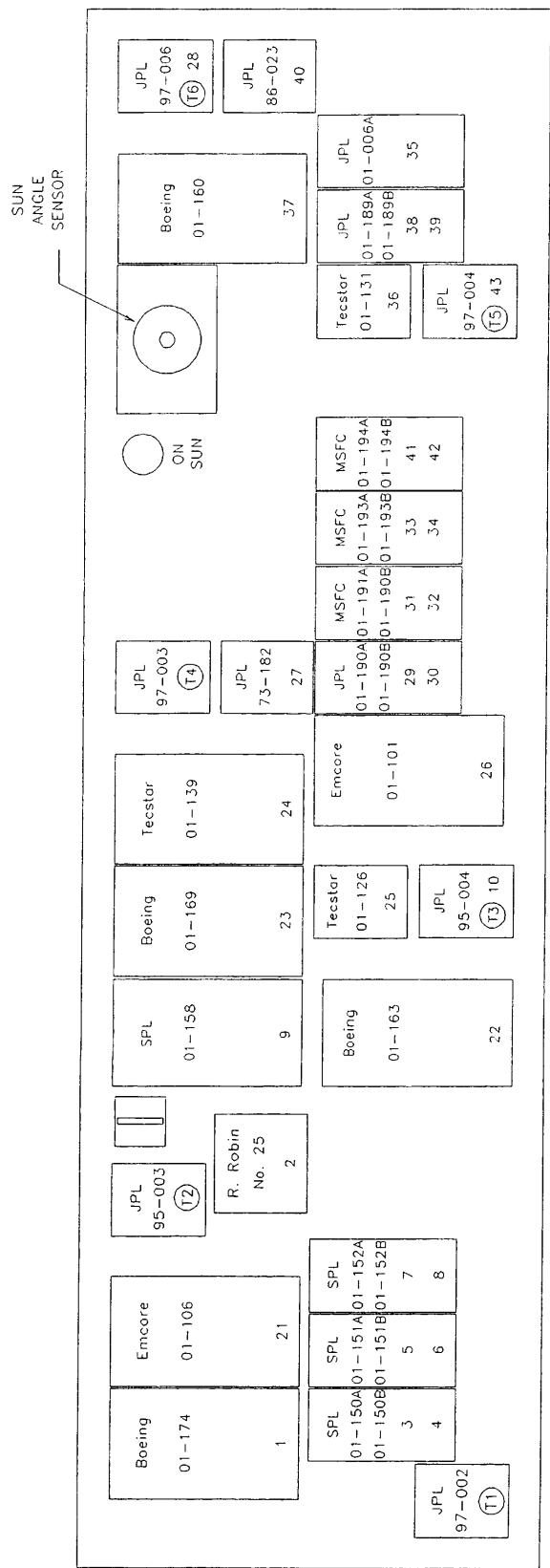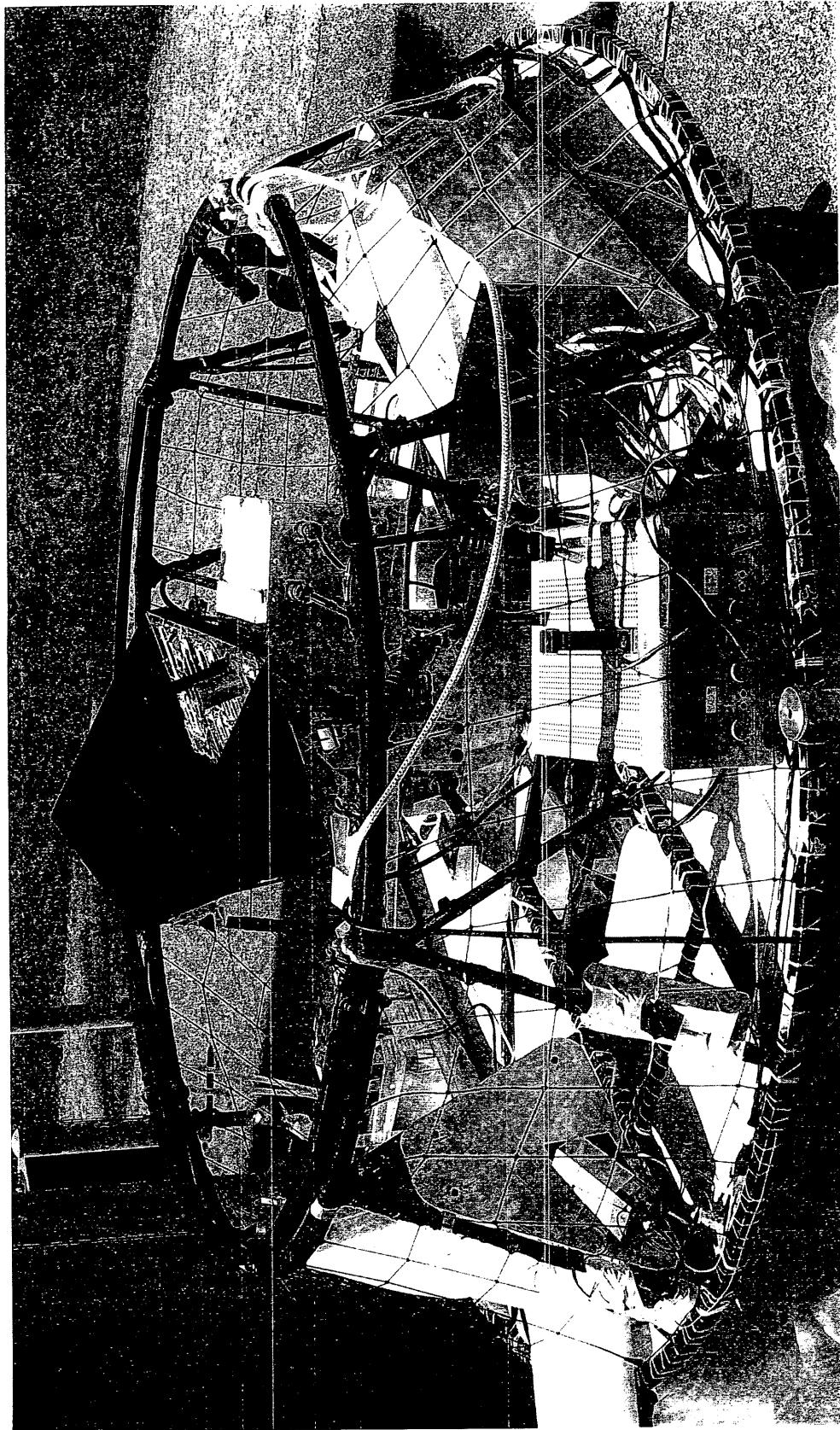The balloon alone weighs 664 lb (301 kg). It is designed to lift itself and a payload weight of up to 725 lb (330 kg), distributed between the bottom and top payloads, to a float altitude of 120,000 ft (36.6 km). At float altitude, the balloon has a diameter of roughly 213 ft (65 m) and a height of 146 ft (45 m). The balloon is built with an internal rip line designed to rip a hole in the side of the balloon for termination of the flight. A special structure is built into the top of the balloon for attaching the top payload. The payload is attached to this structure by means of a stainless steel cable. At flight termination time, a command is sent to cut the cable, allowing the payload to fall away from the balloon.

Trying to inflate and launch a balloon with a sizable weight attached to its top is very awkward and may be likened to trying to balance a beer bottle on a soda straw. A tow balloon tied to the top payload was used during the inflation and launch phases to add stability and to keep it on top. This smaller balloon, about 2,900 ft³ (82 m³), is designed to lift about 180 lb (82 kg). The tow balloon was cut loose from the top payload after the launch as soon as the main balloon stabilized and the launch-induced oscillations damped out.

3.2 TOP PAYLOAD

The top payload consists of the tracker, solar panel, voltage reference box, multiplexer, data encoder, descent parachute, relay box, tracking beacons, telemetry transmitters, command receivers, television camera, and battery power supplies for the tracker, data encoder, receiver, and transmitters. All these items are mounted on the aluminum hoop assembly as shown in Figures 3 and 6. The hoop assembly also serves the following functions:

(1) Permits the top-mounted payload to "float" on top of the balloon and minimizes billowing of balloon material around the top payload.

(2) Serves as the mounting surface that attaches the top payload assembly to the balloon.

(3) Provides a convenient point for attaching the tow balloon and the descent parachute.

(4) Acts as a shock damper to protect and minimize damage to the top payload at touchdown.

The complete apex-mounted hoop assembly, as flown, weighs ≈ 140 lb (63 kg) and descends as a unit by parachute at flight termination.

The Sun tracker, shown in Figures 3 and 6, is capable of orienting the solar panel toward the Sun, compensating for the motion of the balloon and the Sun by using 2-axis tracking in both azimuth and elevation. The tracker has the capability to maintain its lock on the Sun to within ±2 deg. To verify that the tracker was operating properly, the output of an on-Sun indicator was constantly monitored during the flight by feeding its output to the DAQ and entering its signal into the telemetry stream. The on-Sun indicator consists of a small, circular solar cell mounted at the bottom of a collimator tube, 7 in. (17.8 cm) long, with an aperture measuring 0.315 in. (0.8 cm) in diameter. The on-Sun indicator is attached to the solar panel so that it points at the Sun when the panel is perpendicular to the Sun. The output of the on-Sun indicator falls off very rapidly as the collimator tube points away from the Sun and provides a very sensitive indication of proper tracker operation. A Sun-angle-sensor, added to the system in 1996, gives a quantitative readout of the tracker's pointing accuracy.

A reflection shield is attached to the panel to prevent any stray reflected light from reaching any of the modules. This shield is made of sheet aluminum, painted velvet black, and attached to 3 edges of the solar panel.

Since the second 2000 flight, the solar cell modules have been mounted onto the Sun tracker platform with an interface of crinkled aluminum foil, and held in place with 4 screws. The aluminum foil is used to achieve a highly conductive thermal contact between the modules and the panel and to smooth out the temperature distribution over the solar panel as much as possible. The foil appears to provide a thermal interface as good as or better than the vacuum grease previously used, and it eliminates the mess associated with the grease.

The solar panel temperature is monitored using platinum resistance sensors (RTDs). Some of the solar cell modules are constructed with RTDs embedded in the metal substrate directly beneath the solar cell. Six of these modules are mounted on the solar panel at equally spaced locations so that their temperature readings give an accurate representation of panel temperature. Placement of these modules on the 2 flight panels is shown in Figures 2 and 5. A seventh RTD is mounted inside the DAQ to monitor its temperature during environmental testing and during the flight.

A tracking or locator beacon was attached to the hoop assembly. This beacon, similar to those used for tracking wild animals in their natural habitat, consists of a low-wattage transmitter that sends short, 168-MHz pulses at the rate of about 1 per second. A handheld directional antenna and a battery-powered receiver are used inside the chase plane and on the ground for locating the transmitter. This beacon has been very useful in locating this very small payload in a very large open range.

3.3 BOTTOM PAYLOAD

The bottom payload was entirely furnished by the NSBF. It consists of a battery power supply, a ballast module for balloon control, a terminate package, and an electronics module known as the consolidated instrument package (CIP).

Power for operating most of the electrical and electronic equipment on the balloon is supplied by a complement of high-capacity lithium batteries. This supply, furnishing 28 Vdc regulated power and 36 Vdc unregulated power, powered all the instruments in the CIP. Several other small battery sources were used at various locations on the balloon for instruments that require small amounts of power. For example, the tracker and data encoder, the tracking beacons, the TV camera, and the payload telemetry system all have individual battery power supplies. All batteries are sized to supply power for at least twice the expected duration of a normal flight.

High-altitude balloons tend to lose helium slowly during the course of the flight. As a consequence, a helium balloon will tend to reach float altitude and then begin a slow descent. To counteract this tendency, a ballast system is included as part of the bottom payload. It usually contains ≈ 100 lb (45 kg) of ballast in the form of very fine steel shot. The shot may be released in any desired amount by radio command. By proper use of this system, float altitude may be maintained to within ±2,000 ft (±600 m).

The telemetry system in the CIP sends all data transmissions concerning the flight except those for the top payload over a common RF carrier. The CIP also contains a command system for sending commands to the balloon for controlling the housekeeping functions, such as releasing ballast and turning the transponder on and off. Specifically, the CIP contains the following equipment:

(1) Pressure transducers
(2) Subcarrier oscillators, as required

(3) An L-band FM transmitter
(4) A transponder for air traffic control tracking
(5) A pulse code modulation (PCM) command receiver-decoder
(6) Two GPS receivers

The altitude of the balloon is measured with a capacitance-type electronic transducer, manufactured by MKS Instruments, Inc., which reads pressure within the range of 1,020 to 0.4 mbar (102,000 to 40 N/m²) with an accuracy of 0.05%. The transducer produces a dc level that is encoded as PCM data and decoded at the receiving station into pressure, and the altitude is then calculated from the pressure reading. The GPS receivers also compute and send altitude information into the telemetry stream.

The GPS navigation system is used for flight tracking. The second GPS receiver is used as a backup. This system can provide position data to an uncertainty of less than 0.1 mi (0.2 km). The GPS signal is multiplexed into the telemetry stream and updated every 8 seconds.

All the telemetry data is sent to the ground in the form of pulse code modulation. A UHF L-band transmitter in the CIP is used to generate the RF carrier. The L-band carrier is modulated by the pulse code and sent to the receiving station at Palestine.

An aircraft-type transponder was flown so that Air Traffic Control (ATC) could read the balloon's location on their radar systems during the descent portion of the flight. ATC is often helpful in relaying to the recovery aircraft the exact position of the bottom payload during its descent on the parachute.

The purpose of the PCM command systems is to send commands to the balloon; e.g., release the bottom payload from the balloon and release ballast. Like the PCM system used on the top payload, it is designed to reject false commands and is highly reliable in operation. The data is encoded on a frequency-shift-keyed audio carrier. This signal is then decoded into data and timing control. Each command consists of a double transmission of the data word. Both words must be decoded and pass a bit-by-bit comparison before a command can be executed. Commands may be sent to the balloon from either the ground station at Palestine or from the recovery airplane.

The lower payload is suspended from the balloon by a 14-m diameter parachute. The top end of the parachute is fastened to the bottom of the balloon, and the lower payload (which contains the CIP, the battery power supplies, the terminate electronics, and the ballast) is

12

attached to a fitting at the bottom of the shroud lines. Appropriate electrical cables and breakaway connectors are rigged in parallel with the mechanical connections. The whole bottom assembly is designed to break away from the balloon and fall to Earth while suspended from the parachute at termination of the flight.

4. FLIGHT SEQUENCE

4.1 PRELAUNCH PREPARATIONS AND LAUNCH

The balloon launchpad at the NSBF is a large circular area, 2,000 ft (600 m) in diameter. In the center of this large circle is another circular area, solidly paved, measuring 1,000 ft (300 m) in diameter. This circular launchpad allows layout of the balloon in precise alignment with the surface wind. Hay is planted in the area between the 2 circles, and a paved road surrounds the larger circle. Paved radials extend from the perimeter road toward the launchpad.

When all prelaunch preparations had been completed and the staff meteorologist had predicted favorable weather and winds at Palestine and for some 300 mi (480 km) downrange, the equipment was taken to the launch site. (Launches from Palestine are only authorized when the predicted termination point is at least 200 mi west of Palestine.)

At the launchpad, the main balloon, protected by a plastic sheath, was laid out full-length on the circular paved area. It was aligned with the direction of the wind and positioned so that the top of the balloon was on the upwind side. The top end of the balloon was passed under, then around a large, smooth, horizontal spool mounted on the front end of the launch vehicle. One end of this launching spool was hinged to the launch vehicle. The other end of the spool had a latch that could be released by a trigger mechanism. After the balloon was passed over the spool, the spool was pushed back to engage the latch so that the spool trapped the balloon. The top 10 m or so of the balloon was pulled forward from the spool, allowing the top payload to rest on the ground. It is this top 10 m of balloon that later received the helium gas during inflation. After the launching spool was latched, final preparations of the top payload began. The tow balloon was attached to the hoop with nylon lines and a final checkout of the tracker and data encoder was performed.

The launch sequence began by inflating the tow balloon with helium to the point where it just lifted the top payload assembly. The main balloon was then inflated by passing a predetermined volume of helium through 2 long fill-tubes and into the balloon. The helium formed a bubble in the part of the balloon above the launching spool. Figure 7 shows the configuration of the flight train at this stage of preparation. The balloon was launched by triggering the latch on the launching spool. When the latch was released, a stout spring caused the free end of the spool to fly forward, rotating about the hinge, which released the balloon. As the balloon rose, the second launch vehicle at the lower end of the balloon began to move forward (downwind). After the driver of the second launch vehicle had positioned the vehicle directly below the balloon and had his vehicle going along at the same speed as the balloon, he released the latch on the pin and the lower payload was released. Figure 8 shows the balloon system and the launch vehicle a few seconds after release of the launching spool just as the downwind launch vehicle began to move. As soon as the main balloon quit oscillating, a signal was sent from the launchpad that triggered the explosive charges on the ropes connected to the tow balloon. This released the tow balloon, and the launch sequence was complete.

4.2 FLIGHT

In the 2001 flights, the balloons ascended at a rate of ≈ 900 ft/min (4.6 m/s) and reached float altitude after ≈ 2 hours. During the ascent, the flight controller at Palestine maintained a constant contact with ATC. Data from the onboard navigational system was continuously given to ATC so that air traffic in the area could be vectored around the balloon.

After the balloon was launched (and during flight preparation), solar cell voltages interspersed with reference calibration voltages and RTD voltages were fed into the telemetry system. These voltages were converted to PCM and were transmitted to the NSBF ground station along with the position, altitude, and other information from the CIP. At the ground station, the signals were decoded, recorded, and displayed in real time for monitoring the flight. The TV link was also used at the ground station to monitor the status of the top payload during the flight.

The first balloon was launched on June 26, 2001, at 14:11 UT (9:11 a.m. local time) and reached float altitude at 16:01 UT. The tracker was first turned on at 15:34 UT at an altitude of $\approx 82,000$ ft prior to reaching float and successfully locked on the Sun. The early turn-on permitted the acquisition of solar cell data while the cells were still relatively cool ($\approx 35°C$). The system continued tracking and sending data until 19:08 UT, when the
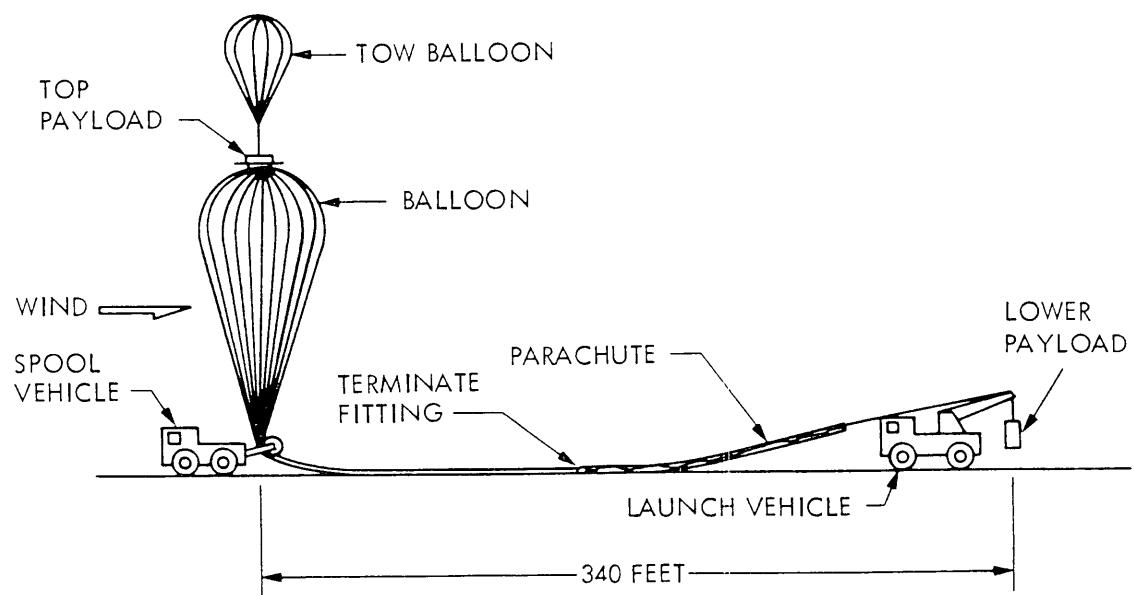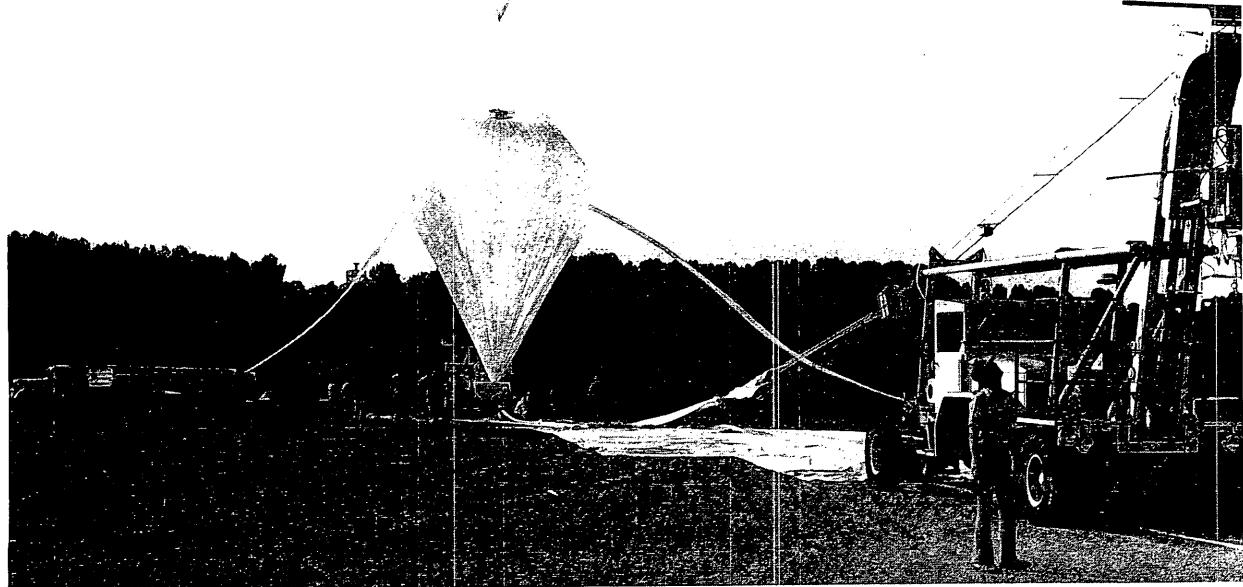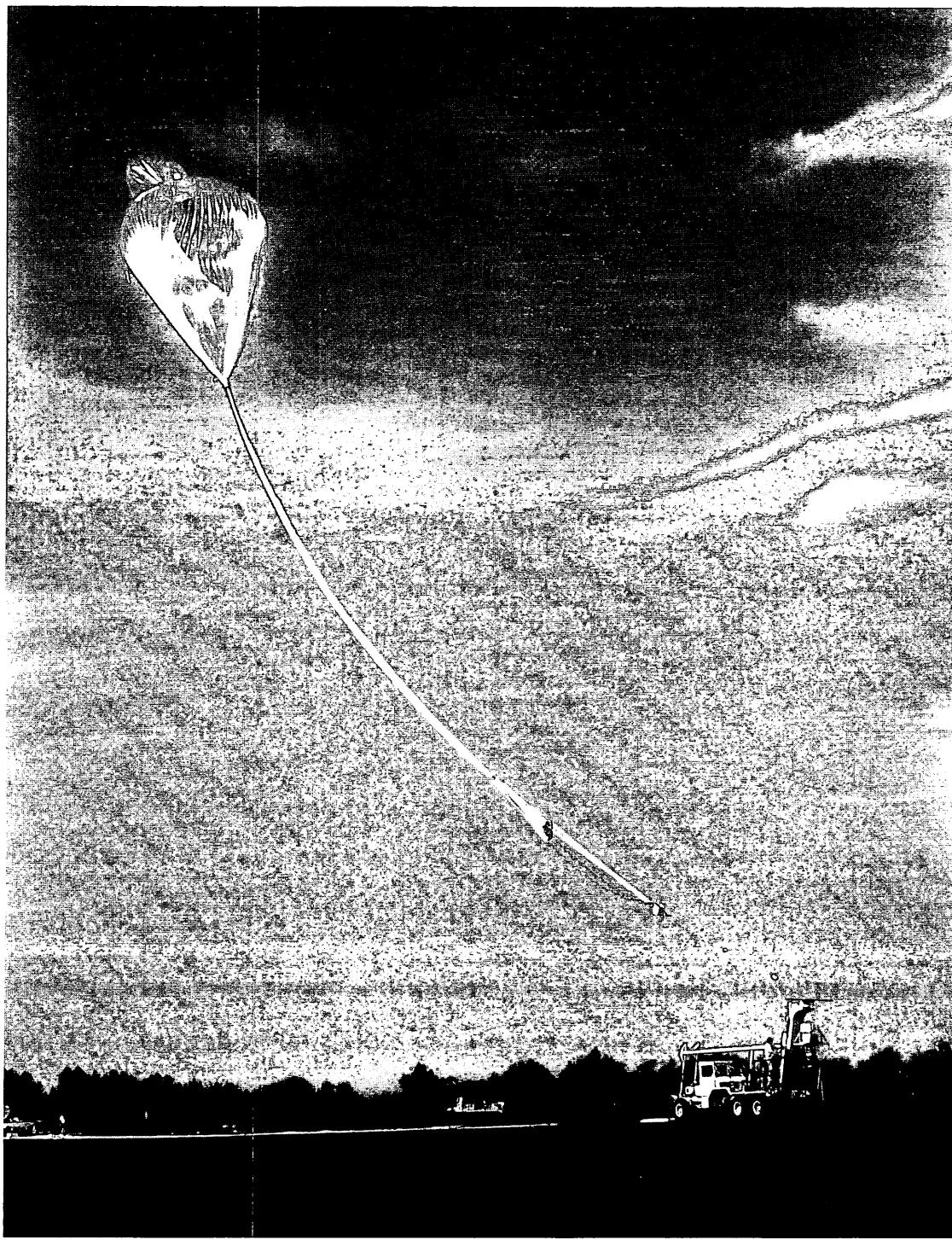
13

Figure 7. Flight Train Configuration

Figure 8. Balloon Launch

tracker was turned off in preparation for termination. The flight was terminated at 19:22 UT.

The second balloon was launched on July 4, 2001, at 14:00 UT (9:00 a.m. local time) and reached float altitude at 16:15 UT. The tracker was turned on and locked on the Sun at 15:31 UT, when it was at an altitude of 80,000 ft. The tracker operated normally and telemetry data was received through 18:45 UT. The flight was terminated at 18:53 UT.

4.3 FLIGHT TERMINATION

Shortly after each launch, a ground recovery crew began driving toward the expected termination area in a special recovery truck. Approximately 2 hours after the balloon reached float altitude, the recovery airplane took off from Palestine with an experimenter and an observer aboard. This airplane was equipped with a telemetry receiver and a computer-controlled system that allowed the crew to monitor the location of the balloon and the status of its systems. Radio equipment aboard the airplane allowed communication with the balloon base and with the ground recovery crew. The airplane also had a full command system so that it could send commands to the balloon.

During the summer months, the winds at altitudes above 80,000 ft (24 km) blow from east to west at speeds of about 50 knots (25 m/s), so the airplane had to fly about 200 mi (330 km) west of Palestine to be in position for recovery. The pilot could fly directly toward the balloon at any time by flying toward the telemetered location of the balloon. This position information was generated by the GPS system on the balloon, telemetered to the balloon base at Palestine, and relayed from there to the airplane. The observer in the recovery airplane shared the responsibility for termination of the flight with the launch director in the NSBF control tower at Palestine. Before leaving Palestine, the recovery personnel had received a set of descent vectors from the meteorologists. The descent vectors are estimates of the trajectories that the payloads should follow as they descend by parachute. Upon receiving word that the experimenter had sufficient data, the pilot flew under the balloon to double-check the accuracy of the GPS data. Using the descent vectors, he then plotted where the payloads should come down. He also established contact with ATC. When ATC advised that the descending payloads would not endanger air traffic, and when the descent vector plots showed that the payloads would not come down in an inhabited area, the flight director at NSBF sent the commands to the balloon that terminated the flight.

The termination sequence began with a command to the balloon that disconnected power from the tracker and data encoder. Next, a command was sent that cut the cable holding the top payload onto the top of the balloon. The third command released the bottom parachute from the balloon, which allowed the bottom payload to fall away and caused the balloon to become top-heavy. As the bottom payload fell, a rip line, connected from the parachute to the body of the balloon, ripped open the side of the balloon. The balloon collapsed, the top payload fell off the balloon, its parachute opened, and all 3 objects began their descent.

Typical descent time for the top payload is ≈40 minutes with its present weight and with a 24-ft (7.32-m)-diameter parachute. The descent time for the bottom payload is ≈60 minutes. While the payloads were descending, the pilot monitored the position of the top and bottom payloads by visual reference. Both payloads were observed from the air at impact and their positions logged using an onboard GPS receiver. The ground recovery crew was directed to each impact site by the pilot as he circled the area in the airplane. This year both descents were normal, and no damage to the solar cells or to the tracker occurred.

This year the touchdown site for the first flight was near Bronte, Texas, ≈230 mi (370 km) from Palestine. The total flight duration from launch until execution of the terminate command was ≈5.2 hours.

The touchdown site for the second flight was ≈17 mi. northeast of Sterling City, Texas, ≈302 mi (486 km) from Palestine. Flight duration from launch until termination was ≈4.9 hours.

5. DATA ANALYSIS

The computer analysis was performed at JPL using a TBASIC (registered trademark of the TransEra Corp.) program written for a PC. The program read the raw data from the files produced by the LabVIEW program during the flight, then corrected the fixed-load cell data for temperature and Earth-Sun distance to a temperature of 28°C and to an Earth-Sun distance of 1 astronomical unit (AU) using the following formula:

16

$$V_{28,1} = V_{T,R}(R^2) - A(T - Tref)$$

$V_{T,R}$ = measured module output voltage at temperature T and distance R, where

R = Sun-Earth distance in AU. (See reference 2)

A = module output temperature coefficient.

T = module temperature in degrees C.

Tref = Standard temperature (usually 28°C).

A similar correction is made to the cells producing I-V curves. The correction shown above is made for all measured cell current values. A separate correction, utilizing a temperature coefficient appropriate for V_{oc}, is applied to the cell voltages, but the factor for Earth-Sun distance is not used. This correction is made for all measured cell voltage values.

The analysis program includes the ability to compute temperature coefficients of the fixed-load cells and of the I_{sc} and V_{oc} of the I-V cells from the flight data. The cell output, corrected only for Earth-Sun distance, was used for these calculations. Data from the RTDs, mounted in 6 of the flight modules, was used for the temperature measurements.

Figure 9 is a plot of cell output vs temperature for module 01-139 on the second flight; this plot consists of 3781 data points. This cell is fitted with a shunt resistor of 0.17 ohms. The plot shows that the cell output is slightly nonlinear and is representative of the temperature dependence of all the cells measured on this flight. A linear least squares fit to the data is shown on the plot, and it illustrates that the linear fit is not quite appropriate. Figure 10 is a plot of the same cell's output, but over a limited temperature range, between 30 and 52°C. This plot consists of 524 data points. A linear least squares fit to this data is also shown and is seen to be quite good. The above observations are also true for the Ge (or bottom cells). The Ge cells exhibited a nonlinear temperature dependence of I_{sc} except that the slopes were generally negative in contrast to the positive slopes of all other cells. A linear temperature coefficient derived over the same lower temperature range worked well for the Ge cells as well.

We therefore used the linear fit over the limited temperature range to derive the I_{sc} temperature coefficient for each cell on the flight (fixed load and I-V cells), and for the V_{oc} temperature coefficient for the I-V cells. Only the data over the 30 — 52°C temperature range was used to derive calibration values for the cells.

The program was modified in 1999 to calculate the gain of the fixed-load-cell amplifiers each time a line of data was read. The known, stable voltages from the external voltage reference source were used as input, and the telemetered output values were used in a linear least squares fit to calculate the gain and offset of the amplifiers in real time.

The program was again modified in 2000 to allow the option of calculating the gain of the fixed-load-cell amplifier using internal calibration voltages of ≈50 and 90 mV built into the DAQ. This option also permits calculating the gain and offset of the amplifier continuously during the flight.

The remainder of this section describes the details of performing the above corrections and computing calibration values for the cells.

5.1 DATA STREAM DESCRIPTION

The data is sent from the computer on the balloon to the ground telemetry station in groups called frames. Each frame consists of 26 lines of data, and each line contains 43 words of data. The first line of data contains the frame synch word, a line count word, a frame count word, time of day, temperature data, calibration voltages, power supply voltages, the on-Sun indicator reading, and a checksum word. The next 25 lines begin with a line synch word and a line count word. In line 2, this is followed by 30 data words corresponding to the outputs of the fixed-load cells (channels 21 through 50). Words 33 through 42 contain fill data (7s), and word 43 is a checksum. The fixed-load cell readings are repeated 4 more times and sent in lines 3 through 6 using the same format as used in line 2. Line 7 begins with the line synch word and a line count word. Words 3 and 4 contain the voltage and current readings resulting from the first load resistor applied to cell 1. The next 38 words contain the voltage and current readings for the remaining 19 loads applied to cell 1. Word 43 is again a checksum. Lines 7 through 26 contain data for the 19 I-V cells and the calibration channel in this same format. The LabVIEW program receives the data in this format and, after producing a real-time display on the computer screen, stores the data on files as it is received.

5.2 FIXED-LOAD CELLS

The computer analysis program performed its analysis in 2 steps. In the first step the cells with fixed loads were read from the files created by the LabVIEW program during the flight. The program began by looking for the frame synch word marking the beginning of a frame.

17

Once this word was found, the on-Sun indicator reading was decoded. If this reading was greater than the minimum allowable value (OSIMIN), analysis proceeded by applying the Earth-Sun distance and temperature corrections to the data for each of the 23 fixed-load cells. Appropriate data for each cell (sums, sums of squares, number of readings, etc.) was accumulated for computing averages, standard deviations, and temperature coefficients after all the data was read.

The temperature for each cell was computed by weighting the values of the 6 RTDs (T1 through T6) on the panel. That is, if cell x was located physically on the panel midway between RTDs T1 and T2, and if T1 and T2 were both mounted under the same cell types as cell x, then the temperature for cell x would be taken to be an equally weighted average of T1 and T2. But if T1 was under a different cell type than that of cell x, then the temperature of cell x might more accurately be computed by applying a higher weighting factor to T2 than to T1. A certain amount of judgment was required of the analyst in choosing the weighting factors involved in the temperature readings. This is of some importance, since the RTDs typically show a temperature gradient over the panel of $\approx 4°C$.

The analysis of the flight data for the fixed-load cells on the first flight revealed that there was something wrong with the data. The temperature dependence of the data was erratic, and we were unable to find a way to extract meaningful and accurate calibration values. We believe there may have been interference from the television transmitter during the flight. The I-V cell data behaved normally, however. On the second flight, data points were accepted between 15:30 and 16:03 UT, while the balloon floated above 80,000 ft and the temperature ranged between 30 and 52°C. A minimum of 524 readings for each fixed-load cell was accepted. Averages and standard deviations were computed for each cell. The results for the flight are reported in Table 1.

5.3 I-V CHARACTERISTIC MEASUREMENTS

The second step in the computer analysis was to extract the data from the I-V cells. The I-V cell data in the first flight behaved normally without the interference problem experienced by the fixed load cells. In this procedure, the frame synch word was found, then the on-Sun indicator reading and the cell temperatures, just as in the procedure for the cells with fixed loads. If the on-Sun indicator reading was at or above the OSIMIN threshold level and the Sun-angle-sensor readings were below the pointing error limits, the current-voltage pairs for each cell were read. The currents were corrected for Earth-

Sun distance and for cell temperature, as described for the fixed-load cells, except that this correction was applied to every current reading using the measured temperature coefficient for I_{sc}. A correction was also made to all the voltage readings using a V_{oc} temperature coefficient appropriate for each cell, but no Earth-Sun correction was made for the voltage values. The temperature coefficients used were those measured during the early part of the flight when the cell temperatures were between 30 and 52°C, as was done for the fixed load cells. The application of the current and voltage corrections is equivalent to a translation in the current and voltage axes. The data for each cell was recorded on a diskette in spreadsheet-compatible format and sent to the supplier of that cell.

5.4 CALIBRATION RESULTS

Table 1 reports the calibration values of the fixed-load cells calibrated on the second 2001 balloon flight, corrected to 28°C and to 1 AU (1.496×10^8 km). The table also reports the standard deviation of the measurements, the preflight and postflight readings of each module in the X25 simulator, and a comparison of the preflight and postflight simulator readings. The simulator intensity was set with a standard cell judged to match the spectral response of the particular balloon flight cell under test. Since we don't know how well the older balloon flight cells used to set the simulator match the spectral response of the newer cells flown, no conclusions should be draw if the pre- or postflight simulator readings do not closely match the readings from the balloon. The purpose of the preflight vs postflight measurements is to make sure no damage occurred to the cells as a result of the flight. The table also reports the temperature coefficients that were used for the analysis.

5.5 DATA REPEATABILITY

Several standard modules have been flown repeatedly over the 37-year period of calibration flights. Module BFS-17A, which had flown on 41 flights, was damaged in 1990 and is no longer available. In its history of 41 flights, the BFS-17A calibration values averaged 60.180, with a standard deviation of 0.278 (0.46%). In addition to giving a measure of the consistency of the year-to-year measurements, BFS-17A also provided insight into the quality of the solar irradiance falling on the solar panel, with regard to uniformity, shadowing, or reflections. This cell had been mounted in various locations on the panel over the years. Nevertheless, its readings were always consistent, which verified that there are no uniformity, shadowing, or reflection problems with the geometry of this system.

We have identified a group of solar cells that will be used as replacements for the function served by BFS-17A. Some cells from this group will be flown every year so that we can continue our year-to-year continuity checks. Five cells were flown from this continuity group on the 2001 flights, but only the data from the second flight is useful for the fixed-load cells because of the anomaly discussed above. Data from these cells is presented in Table 2. Cell 73-182 was flown on the 2001 flights for the 23rd and 24th times. The calibration value from the second flight, 67.19, was 0.98% lower than the average of 67.86 established over 22 flights. Cell 86-023, a GaAs cell flown for the 12th time, measured 0.47% below the average. Cell 97-004, a Si cell flown for the 4th time, measured 0.97% below the average. Cell 97-006, a GaAs/Ge cell flown for the 5th time, measured 0.85% below the average. Cell 95-004, a Si I-V cell flown for the 10th time, exhibited an I_{sc} 0.67% below the average on the first flight and 0.80% below on the second flight. This cell's V_{oc} measured 0.47 mV higher than average on the first flight and 1.33 mV below average on the second flight. These differences in I_{sc} appear to arise primarily from the difference of temperature coefficients used in the data correction routine. This is the first year that we were able to get cell measurements with temperatures as low as 30°C, and, as Figures 9 and 10 show, the temperature coefficients derived from low temperature measurements will tend to give lower calibration values for the flight cells.

5.6 I-V MEASUREMENTS

Figures 11 and 12 are the I-V curves of JPL cell 95-004, which was flown on both 2001 flights. Figures 13 through 21 are the I-V curves of cells furnished by Spectrolab. The other I-V data is omitted by request of the sponsors. Although the I-V characteristics were measured many times during the flight, only 1 curve is shown for each cell. This curve is chosen from the family as best fitting the average values measured for I_{sc}, V_{oc}, and P_{max}. Note that the data does not give a true measure of short-circuit current because the curves do not go through 0 volts. This is because the I-V curves are generated by a succession of resistive loads. The resistive load actually consists of a series string of resistances, including the current-measuring resistor (0.1 ohm), the leads from the DAQ to the cells and the load resistor(s) themselves. Even though the load resistance introduced by the program is 0 ohms, the remaining resistances in the string are sufficient to load the cell at a voltage considerably greater than 0 volts. This is particularly true for cells with large areas that produce large currents.

The curves are derived from the digital telemetry data recorded during each flight. Data from the Sun angle sensor was used to select only those curves taken while the tracker was pointed at the Sun to within 3° in azimuth and -2.5° to +2° in elevation for the first flight. The tracker was adjusted better for the second flight and data was acceptable to within ±2° in both azimuth and elevation. This constraint along with the time constraints discussed above resulted in 84 acceptable I-V curves generated on the first flight and 110 acceptable curves on the second flight.

Table 3 displays some statistical data about the curves depicted in the figures. The table gives the mean, the standard deviation, the maximum measured value, and the minimum measured value for 6 of the important cell parameters. These statistics apply only to the curves that fell within the pointing accuracy criteria described above.

6. CONCLUSIONS

The second 2001 balloon flight was successful in all respects. The fixed load cell data from the first flight was unuseable, but the I-V data was good. Both flights were launched at later times than usual, allowing some cell measurements at temperatures near 28° C. Five cells from previous flights were reflown this year. The measurements tend to be a bit lower than those of previous years. We believe this is because the temperature coefficients of the cell parameters derived from the flight data are more accurate than those measured previously. We believe that the agreement is very satisfactory and that the calibration values reported for the 2001 flights can be used with a high degree of confidence.

7. REFERENCES

1. B. E. Anspaugh, R. G. Downing, and L. B. Sidwell, *Solar Cell Calibration Facility Validation of Balloon Flight Data: A Comparison of Shuttle and Balloon Flight Results*, JPL Publication 85-78, Jet Propulsion Laboratory, California Institute of Technology, Pasadena, California, October 15, 1985.

2. *The Astronomical Almanac for the Year 2001*, U.S. Nautical Almanac Office, U.S. Naval Observatory, Superintendent of Documents, U.S. Government Printing Office, Washington, DC 20402, pp. C10–C12.

19

Table 1. Balloon Flight 7/04/01 120,000 Ft. RV = 1.0166422 Flt. No. 1576P

		MODULE CALIBRATION DATA			COMPARISON SOLAR SIMULATOR & FLIGHT				GENERAL INFORMATION
		Temp			Pre-Flt vs Post-Flt Comparison		Post-Flt.		
		Intensity			AMO, Solar Sim.		vs	Temp.	
Module		Adjusted	Std		1 AU 28 Deg C.		Pre-Flt.	Coeff.	
Number	Org.	Average	Dev		Pre-Flt	Post-Flt	(Percent)	(mV/C)	Comments
01-160	Boeing	89.22	0.2283		92.09	93.51	1.54	0.12940	Top Cell Not Irr
01-163	Boeing	92.77	0.0759		93.09	94.49	1.50	0.08390	ITJ, Mid, Not Irr
01-169	Boeing	86.80	0.1106		88.86	89.66	0.90	0.10310	ITJ, Top, Irr
01-101	Emcore	25.95	0.0802		28.15	28.48	1.17	-0.03780	Emcore Ge Sgl Jcn
01-106	Emcore	89.08	0.1257		90.77	91.57	0.88	0.11130	Emcore Top
73-182	JPL	67.19	0.0523		69.90	70.52	0.89	0.07660	HEK 2 ohm-cm
86-023	JPL	58.47	0.0855		59.88	60.12	0.40	0.06080	ASEC GaAs Mantech
97-004	JPL	88.89	0.0591		91.38	91.32	-0.07	0.08010	ASE Si 10 ohm-cm T5
97-006	JPL	74.96	0.1949		77.30	77.45	0.19	0.08220	SPL GaAs T6
01-06A	JPL	85.41	0.0658		88.29	87.67	-0.70	0.10070	Tecstar Full Cell
01-189A	JPL	82.95	0.0599		84.92	84.04	-1.04	0.09030	Emcore Full Structure
01-189B	JPL	27.98	0.0333		31.10	31.08	-0.06	-0.01510	Emcore Bot Cell
01-190A	JPL	82.59	0.0613		85.21	84.63	-0.68	0.10920	Emcore Top Cell
01-190B	JPL	86.55	0.0706		88.24	87.95	-0.33	0.06960	Emcore Mid Cell
01-191A	MSFC	81.79	0.0663		84.74	84.02	-0.85	0.09420	Emcore Full Cell
01-191B	MSFC	28.35	0.0458		32.27	31.45	-2.54	-0.01830	Emcore Bot Cell
01-193A	MSFC	83.86	0.0705		86.95	86.40	-0.63	0.09940	Tecstar Full Cell
01-193B	MSFC	28.62	0.0755		31.87	29.29	-8.10	-0.09890	Tecstar Bot Cell
01-194A	MSFC	85.81	0.0902		89.58	89.47	-0.12	0.10110	Tecstar Top Cell
01-194B	MSFC	86.71	0.0519		88.61	87.89	-0.81	0.05740	Tecstar Mid Cell
01-126	Tecstar	22.83	0.0210		25.10	24.95	-0.60	-0.03240	Tecstar Bot Cell
01-131	Tecstar	84.51	0.1005		88.30	87.83	-0.53	0.10540	Tecstar Top Cell
01-139	Tecstar	84.62	0.0923		84.85	88.06	3.78	0.10030	Tecstar Top Cell

Table 2. Repeatability of Five Standard Solar Cell Modules Over a 27-year Period

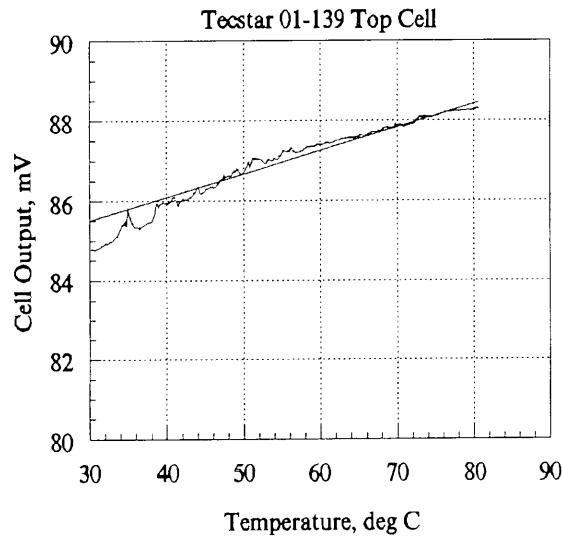| Flight Date	73-182 HEK	86-023 GaAs Mantech	97-004 ASE Si 10Ω-cm	97-006 SPL GaAs/Ge	95-004 ASEC Si Isc	95-004 ASEC Si Voc
4/5/74	68.37					
6/6/75	67.88					
6/10/77	67.96					
7/20/78	68.20					
8/8/79	67.83					
7/24/80	68.00					
7/25/81	67.96					
7/21/82	68.03					
7/12/83	68.03					
7/19/84	67.62					
8/84 Shuttle						
7/12/85						
7/15/86		58.46				
8/23/87		59.47				
8/7/88		58.26				
8/9/89		58.30				
9/6/90		58.89				
8/1/91		59.12				
8/1/92		58.68				
7/29/93	67.71					
8/6/94	67.77	58.91				
8/31/95	67.95	58.69				
6/30/96	67.65	58.51			166.83	617.08
8/8/96	68.26				167.49	617.90
6/11/97	67.66				168.36	614.60
8/2/97	67.53		90.09	75.54		
8/24/97	67.51		89.97	75.26	166.10	623.29
8/15/98	67.84		90.10	75.96		
6/14/99	67.79				166.0	609.1
7/6/99		59.24		76.29	166.0	596.4
6/27/00	68.20				167.0	610.6
7/5/00	68.05				166.4	610.5
6/26/01			88.89		165.4	612.8
7/4/01	67.19	58.47		74.96	165.2	611.0
No. of Meas.	23	12	4	5	10	10
Average	67.869	58.750	89.763	75.602	166.546	612.327
Std. Dev.	0.274	0.383	0.585	0.533	0.969	7.082
Max. Value	68.370	59.470	90.100	76.290	168.36	623.290
Min. Value	67.190	58.260	88.890	74.960	165.210	596.400
Max. Dev.	0.679	0.720	0.872	0.688	1.814	15.927

Figure 9.   Tecstar 01-139: Top Cell vs Temp. for all Flight Data, Flight 01-2 (1576P)
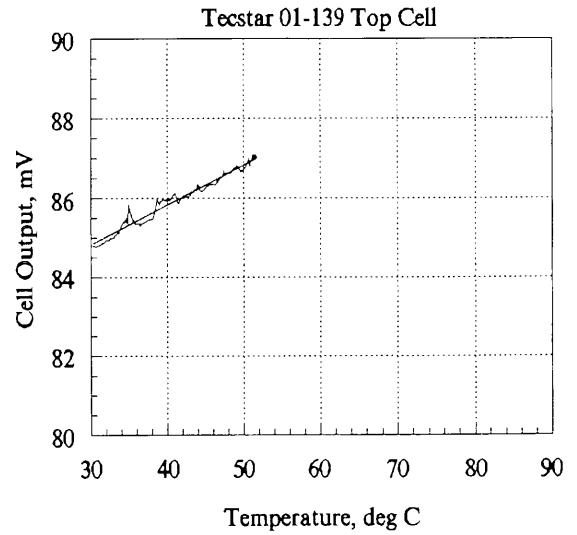

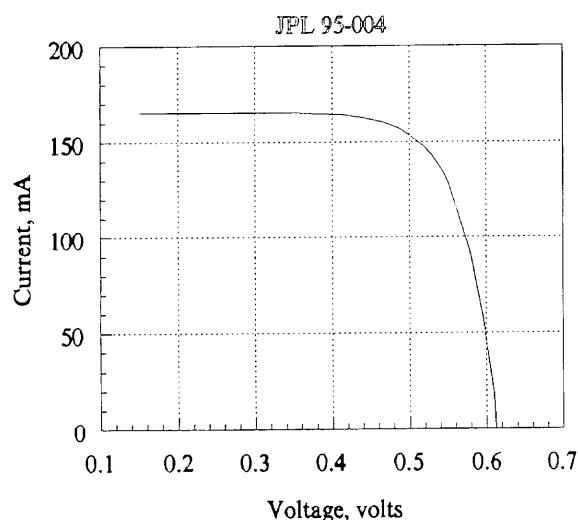Figure 10.   Tecstar 01-139: Top Cell vs Temp. for 30 < T < 52 °C, Flight 01-2 (1576P)

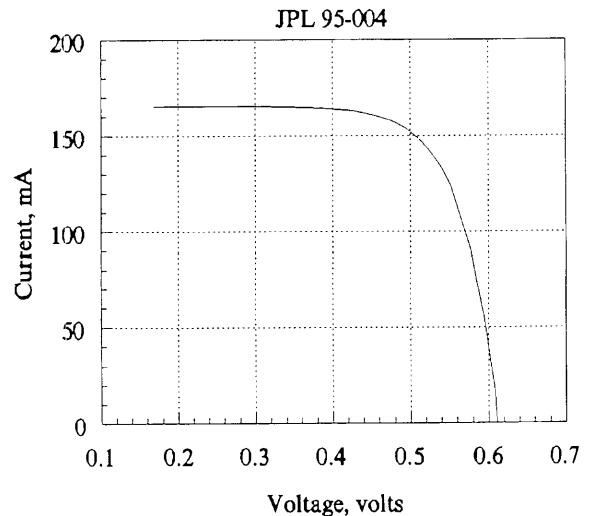Figure 11.   JPL 95-004: ASEC 10Ω-cm, 8 mils, BSFR, Flight 01-1 (1575P)

Figure 12.   JPL 95-004: ASEC 10 Ω-cm, 8 mils, BSFR, Flight 01-2 (1576P)
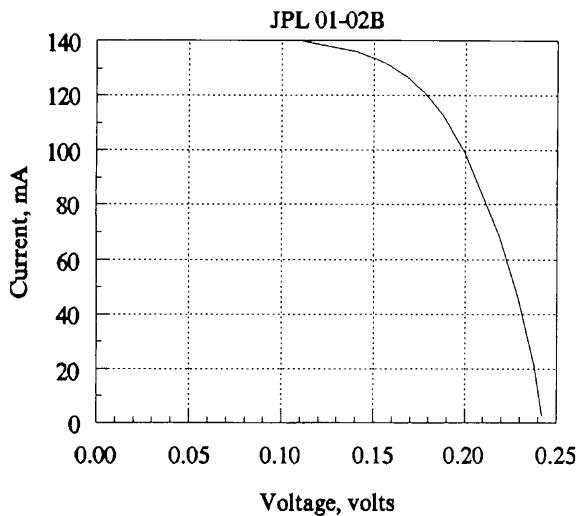
Figure 13. JPL 01-02B: SPL Triple Jcn Cell, Bottom Isotype, Flight 01-1 (1575P)

Figure 14. SPL 01-153: Triple Jcn Cell, Mid Isotype, Flight 01-1 (1575P)

Figure 15. SPL 01-150A: Triple Jcn Cell, Top Isotype, Flight 01-2 (1576P)

Figure 16. SPL 01-150B: Triple Jcn Cell, Mid Isotype, Flight 01-2 (1576P)

Figure 17. SPL 01-151A: Triple Jcn Cell, Top Isotype, Flight 01-2 (1576P)

Figure 18. SPL 01-151B: Triple Jcn Cell, Mid Isotype, Flight 01-2 (1576P)

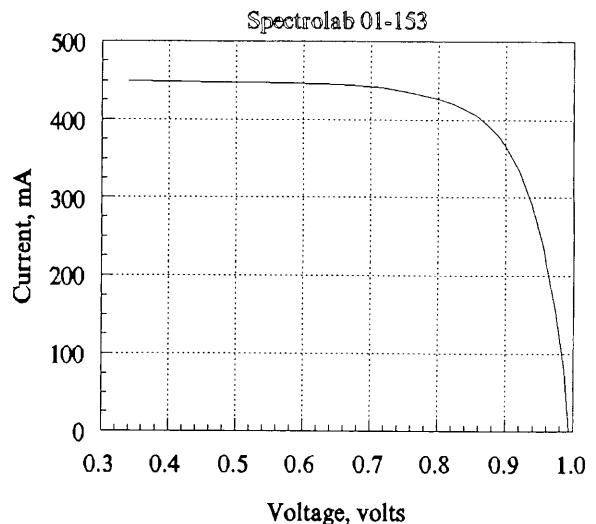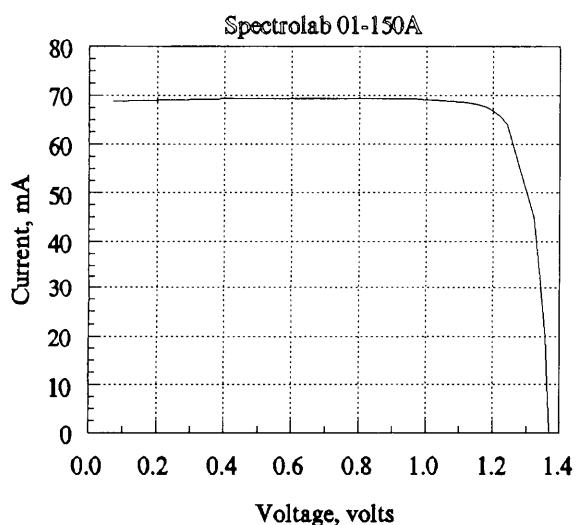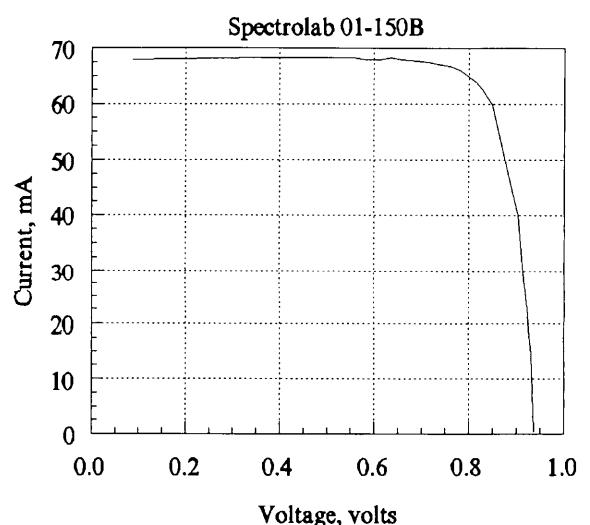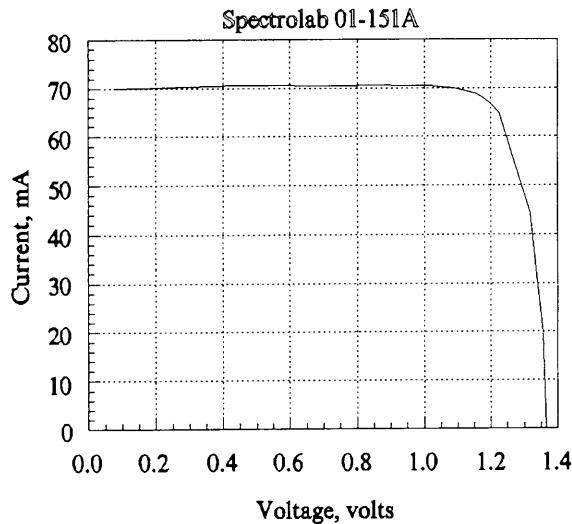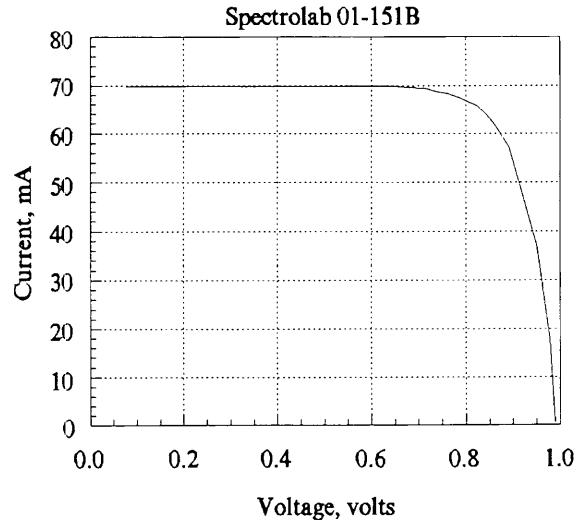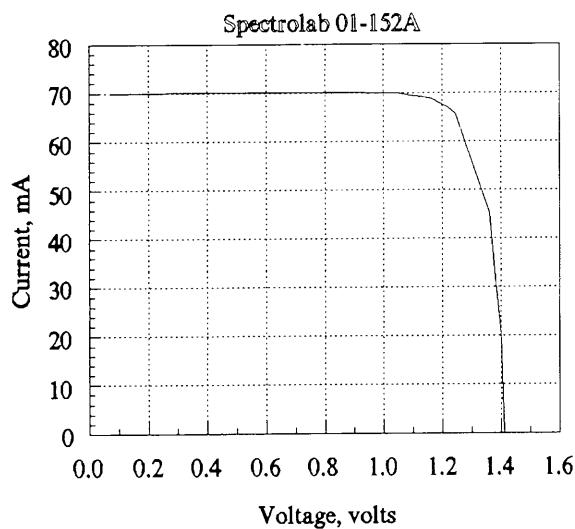Figure 19. SPL 01-152A: Triple Jcn Cell, Top Isotype, Flight 01-2 (1576P)
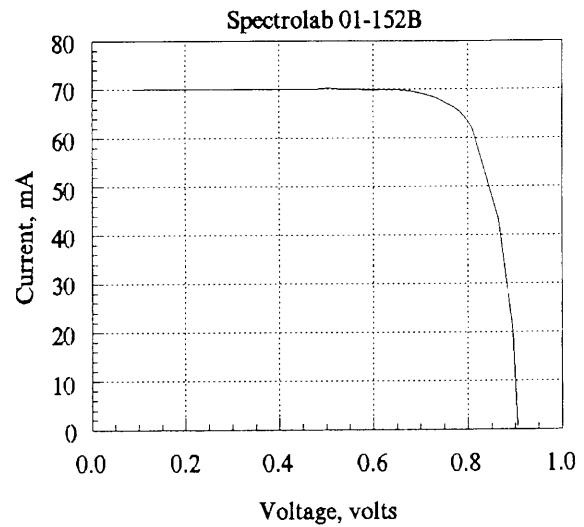

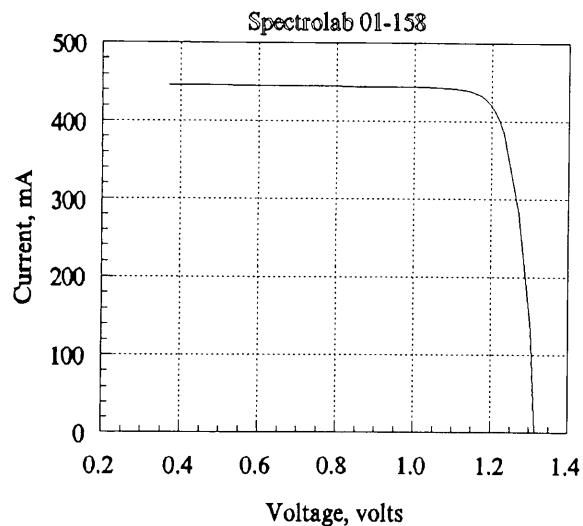Figure 20. SPL 01-152B: Triple Jcn Cell, Mid Isotype, Flight 01-2 (1576P)

Figure 21. SPL 01-158: Triple Jcn Cell, Top Isotype, Flight 01-2 (1576P)

Table 3. Statistical Data for the Cells with I-V Measurements

95-004 (Flight 1, Figure 11)

	I_{sc}	V_{oc}	I_{mp}	V_{mp}	P_{max}	FF
Average	165.4	612.8	152.0	505.6	76.86	0.758
Std. Dev.	0.13	0.39	1.38	3.6	0.22	0.002
Max.	165.7	613.8	155.2	515.2	77.34	0.763
Min.	165.2	611.5	149.6	493.8	76.43	0.754

95-004 (Flight 2, Figure 12)

Average	165.2	611.0	151.6	501.9	76.08	0.753
Std. Dev.	0.15	0.23	1.25	4.33	0.38	0.004
Max.	165.5	611.7	154.3	513.9	77.01	0.763
Min.	164.6	610.3	149.1	493.8	75.54	0.749

01-02B (Figure 13)

Average	139.9	242.1	121.4	176.9	21.47	0.634
Std. Dev.	0.10	3.42	1.38	2.02	.04	0.001
Max.	140.1	243.0	125.0	182.6	21.59	0.638
Min.	139.7	241.5	117.6	171.8	21.40	0.631

01-153 (Figure 14)

Average	449.7	994.0	408.2	849.7	346.83	0.776
Std. Dev.	0.25	0.34	4.36	10.2	1.48	0.003
Max.	450.4	994.8	417.1	858.7	349.58	0.782
Min.	449.1	993.1	402.1	828.6	344.56	0.771

01-150A (Figure 15)

Average	68.84	1369.3	66.3	1207.8	80.05	0.849
Std. Dev.	0.10	0.37	0.45	9.26	0.238	0.003
Max.	69.12	1370.8	67.2	1233.2	80.62	0.856
Min.	68.53	1368.3	64.9	1188.5	79.68	0.844

01-150B (Figure 16)

Average	67.99	937.5	64.2	811.9	52.08	0.817
Std. Dev.	0.09	0.38	0.56	7.62	0.21	0.003
Max.	68.17	938.6	65.4	825.8	52.57	0.825
Min.	67.82	936.1	63.1	798.1	51.76	0.811

Table 3. Statistical Data for the Cells with I-V Measurements (Cont'd)

01-151A (Figure 17)

	I_{sc}	V_{oc}	I_{mp}	V_{mp}	P_{max}	FF
Average	70.00	1366.4	67.3	1186.6	79.88	0.835
Std. Dev.	0.10	0.92	0.43	8.65	0.23	0.003
Max.	70.20	1369.0	68.1	1201.9	80.44	0.844
Min.	69.64	1364.8	66.7	1168.3	79.53	0.830

01-151B (Figure 18)

	I_{sc}	V_{oc}	I_{mp}	V_{mp}	P_{max}	FF
Average	69.91	990.5	64.6	834.6	53.94	0.779
Std. Dev.	0.08	0.98	0.49	6.13	0.27	0.004
Max.	70.12	993.1	66.3	845.6	54.71	0.789
Min.	69.74	988.9	63.8	817.3	53.57	0.773

01-152A (Figure 19)

	I_{sc}	V_{oc}	I_{mp}	V_{mp}	P_{max}	FF
Average	69.89	1410.8	66.1	1235.4	81.67	0.828
Std. Dev.	0.10	0.77	0.37	6.94	0.10	0.001
Max.	70.12	1413.6	67.35	1251.9	81.89	0.834
Min.	69.60	1409.3	65.3	1212.0	81.46	0.825

01-152B (Figure 20)

	I_{sc}	V_{oc}	I_{mp}	V_{mp}	P_{max}	FF
Average	70.08	905.9	65.6	780.3	51.17	0.806
Std. Dev.	0.09	0.90	0.37	4.73	0.17	0.003
Max.	70.25	909.1	66.9	790.3	51.69	0.814
Min.	69.74	904.4	64.9	764.9	50.93	0.801

01-158 (Figure 21)

	I_{sc}	V_{oc}	I_{mp}	V_{mp}	P_{max}	FF
Average	445.9	1316.8	430.4	1179.3	507.53	0.864
Std. Dev.	0.47	1.19	2.03	6.33	1.45	0.002
Max.	447.6	1319.9	434.7	1191.7	511.90	0.870
Min.	444.8	1314.2	426.6	1164.7	505.81	0.861

REPORT DOCUMENTATION PAGE

Public reporting burden for this collection of information is estimated to average 1 hour per response, including the time for reviewing instructions, searching existing data sources, gathering and maintaining the data needed, and completing and reviewing the collection of information. Send comments regarding this burden estimate or any other aspect of this collection of information, including suggestions for reducing this burden, to Washington Headquarters Services, Directorate for Information Operations and Reports, 1215 Jefferson Davis Highway, Suite 1204, Arlington, VA 22202-4302, and to the Office of Management and Budget, Paperwork Reduction Project (0704-0188), Washington, DC 20503.

1. AGENCY USE ONLY *(Leave blank)*	2. REPORT DATE 02/01/2002	3. REPORT TYPE AND DATES COVERED JPL Publication

4. TITLE AND SUBTITLE
Results of the 2001 JPL Balloon Flight Solar Cell Calibration Program

5. FUNDING NUMBERS
C - NAS7-1407
Project: 101451
Task: 01.01

6. AUTHOR(S)
B. E. Anspaugh
R. L. Mueller

7. PERFORMING ORGANIZATION NAME(S) AND ADDRESS(ES)
Jet Propulsion Laboratory
California Institute of Technology
4800 Oak Grove Drive
Pasadena, CA 91109-8099

8. PERFORMING ORGANIZATION REPORT NUMBER
JPL Publication 02-004

9. SPONSORING / MONITORING AGENCY NAME(S) AND ADDRESS(ES)
National Aeronautics and Space Administration
Washington, DC 20546-0001

10. SPONSORING / MONITORING AGENCY REPORT NUMBER
--

11. SUPPLEMENTARY NOTES
--

12a. DISTRIBUTION / AVAILABILITY STATEMENT

SUBJECT CATEGORY: 44 Energy Production and Conversion   DISTRIBUTION: Nonstandard

AVAILABILITY: NASA CASI (301) 621-0390

12b. DISTRIBUTION CODE
--

13. ABSTRACT *(Maximum 200 words)*
The 2001 solar cell calibration balloon flight campaign consisted of two flights, which occurred on June 26, 2001, and July 4, 2001. Fifty-nine modules were carried to an altitude of approximately 120,000 ft (36.6 km). Full I-V curves were measured on nineteen of these modules, and output at a fixed load was measured on thirty-two modules (forty-six cells), with some modules repeated on the second flight. Nine modules were flown for temperature measurement only. The data from the fixed load cells on the first flight was not usable. The temperature dependence of the first-flight data was erratic and we were unable to find a way to extract accurate calibration values. The I-V data from the first flight was good, however, and all data from the second flight was also good. The data was corrected to 28 degrees C and to 1 AU (1.496 E8 km). The calibrated cells have been returned to their owners and can now be used as reference standards in simulator testing of cells and arrays.

14. SUBJECT TERMS
solar cells; photovoltaic cells; balloon flight;calibrating; modules

15. NUMBER OF PAGES
27

16. PRICE CODE
--

17. SECURITY CLASSIFICATION OF REPORT	18. SECURITY CLASSIFICATION OF THIS PAGE	19. SECURITY CLASSIFICATION OF ABSTRACT	20. LIMITATION OF ABSTRACT
Unclassified	Unclassified	Unclassified	Unlimited

NSN 7540-01-280-5500   JPL 2659 5 / 99 FF   Standard Form 298 (Rev. 2-89)
Prescribed by ANSI Std. Z-39-18
298-102